inherits the symmetry of the Hamiltonian, and any user-supplied initial condition is symmetric by definition with respect to the spins that the user had declared equivalent.

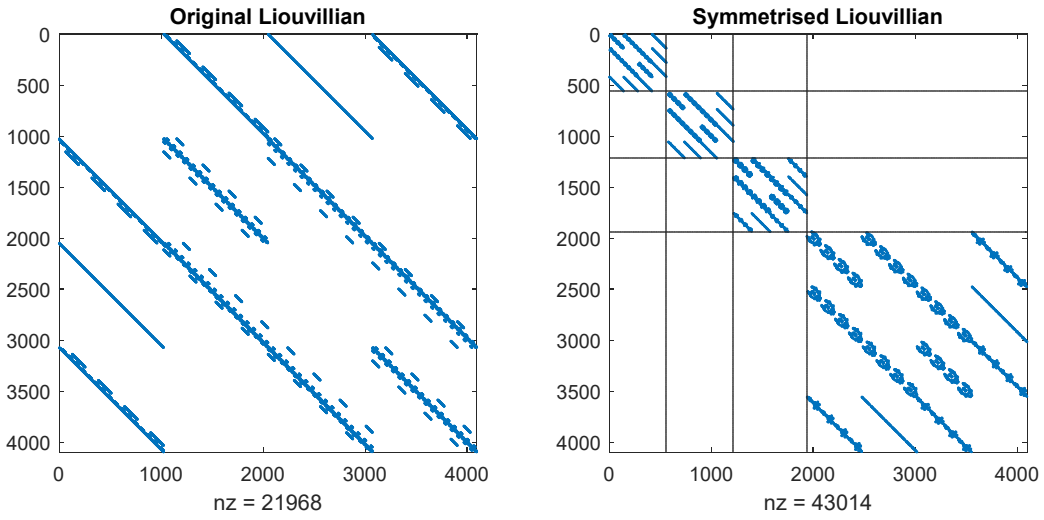

Figure 10. *Block structure emerging in the spin Hamiltonian commutation superoperator (Liouville space) of a radical pair with four equivalent spin-1/2 nuclei after symmetry factorisation under the S_4 permutation group. Blue dots indicate non-zero elements. The Liouvillian includes isotropic Zeeman interactions for all particles and equal isotropic hyperfine couplings between one of the electrons and the four nuclei. Only the fully symmetric irreducible representation block (top left) is populated unless the symmetry is broken and subsequently restored.*

Thus, in Liouville space, SALCs of basis operators not belonging to the fully symmetric irrep of the system symmetry group may be dropped from the basis because they do not get populated. The construction of fully symmetric SALCs is efficient because all characters of the fully symmetric irrep are equal to 1:

$$\mathbf{O}_k^{(\mathrm{A_{1g}})} = \frac{1}{N}\sum_{g\in G} g\left(\mathbf{O}_k\right) \tag{595}$$

The resulting Liouville space dimension reduction factor is equal to the order of the group. In the rare situations where other irreps are populated (*e.g.* by user's decision in the initial condition) and therefore must be tracked in Liouville space, there is still a significant efficiency gain because the Liouvillian is block-diagonal (Figure 10) in the symmetry-adapted basis.

4.6.3 Total spin representation

Another approach to symmetry factorisation stems from the total spin representation. For a given set of identical spins, the direct product representation of their algebra may be reduced by diagonalising the Casimir operator (Section 1.5.12) and one of the three generators, conventionally $\mathbf{S}_Z$. The procedures are described in Section 2.5; they are only efficient when the factorisation is applied to each subset of identical spins *before* the direct product representation for the entire spin system is constructed. Factorisation by the total spin achieves the same final result of block-diagonalising the Hamiltonian operator (Hilbert space) and commutation superoperator (Liouville space).

4.7 Product operator formalism

Magnetic resonance spectroscopy has a powerful semi-analytical formalism that provides physical insight into time-domain spin dynamics and enables straightforward analysis of common experiments [125]. It

uses the fact that density matrix can be eliminated from the equation of motion, and the time dynamics problem reformulated entirely in terms of observables. For a specific observable $O(t)$:

$$\begin{gathered}\frac{\partial}{\partial t}\langle\mathbf{O}\rangle=\mathrm{Tr}\left(\mathbf{O}\left(\frac{\partial}{\partial t}\boldsymbol{\rho}\right)\right)=-i\mathrm{Tr}\left(\mathbf{O}[\mathbf{H},\boldsymbol{\rho}]\right)= \\ =i\mathrm{Tr}\left([\mathbf{H},\mathbf{O}]\boldsymbol{\rho}\right)=i\langle[\mathbf{H},\mathbf{O}]\rangle\end{gathered} \tag{596}$$

where $\mathbf{O}$ is the operator of the observable. Because the interactions in the Hamiltonian have at most two-spin operators, the commutators on the right hand side are straightforward. When some relevant subset of observable operators is chosen, the result is a system of equations not unlike those seen in chemical kinetics – the subject with which chemists have much experience and intuition.

In particular, when the operator basis set is chosen to be direct products of single-spin operators and the interactions present in the Hamiltonian are considered one at a time, the dynamics prescribed by Eq (596) may be represented by simple rotation diagrams. On the educational side, these diagrams are the foundation of magnetic resonance spectroscopy and imaging.

4.7.1 Evolution under Zeeman interactions

Consider the evolution of a single isotropically shielded spin L in a strong and uniform magnetic field directed along the Z axis. The Hamiltonian is just the Zeeman interaction $\omega\mathbf{L}_\mathrm{Z}$, and a convenient basis set are Cartesian spin operators $\{\mathbf{L}_\mathrm{X},\mathbf{L}_\mathrm{Y},\mathbf{L}_\mathrm{Z}\}$. The relevant commutators are just the structure relations of the $\mathfrak{su}(2)$ algebra (Section 1.6.3); placing those into Eq (596) yields:

$$\begin{cases}\dfrac{\partial}{\partial t}\langle\mathbf{L}_\mathrm{X}\rangle=-\omega\langle\mathbf{L}_\mathrm{Y}\rangle \\ \dfrac{\partial}{\partial t}\langle\mathbf{L}_\mathrm{Y}\rangle=+\omega\langle\mathbf{L}_\mathrm{X}\rangle \\ \dfrac{\partial}{\partial t}\langle\mathbf{L}_\mathrm{Z}\rangle=0\end{cases} \tag{597}$$

where $\langle\mathbf{L}_{\{\mathrm{X,Y,Z}\}}\rangle=L_{\{\mathrm{X,Y,Z}\}}$ will be used for observables from now on. Eq (597) is a special case of Bloch equations [94] describing circular precession of the $[L_\mathrm{X}\quad L_\mathrm{Y}\quad L_\mathrm{Z}]$ vector around the magnetic field vector. This may be seen from the solution produced by $L_\mathrm{X}=1/2$, $L_\mathrm{Y}=L_\mathrm{Z}=0$ initial condition:

$$L_\mathrm{X}(t)=\tfrac{1}{2}\cos(\omega t),\qquad L_\mathrm{Y}(t)=\tfrac{1}{2}\sin(\omega t),\qquad L_\mathrm{Z}(t)=0 \tag{598}$$

After a similar treatment for the magnetic field directed along X and Y axes of the laboratory frame (corresponding to $\mathbf{H}=\omega\mathbf{L}_\mathrm{X}$ and $\mathbf{H}=\omega\mathbf{L}_\mathrm{Y}$ respectively), the following diagrams summarise the dynamics:

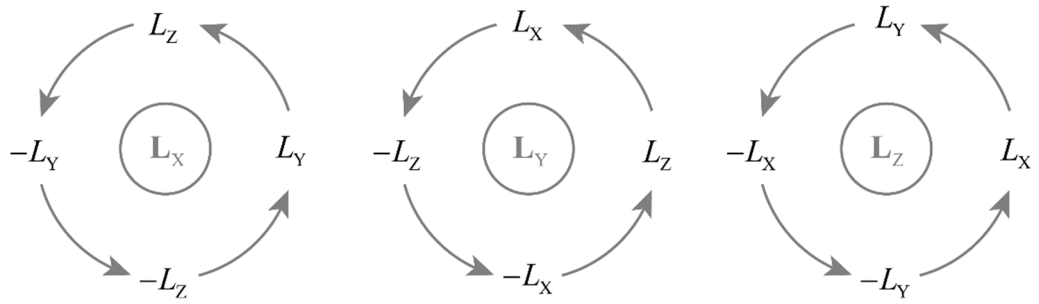

Figure 11. *Exponential action diagrams by SU(2) generators indicated in the circles on the su(2) Lie algebra. Physically, the generators of SU(2) correspond to observable magnetisation operators, and this picture may therefore be interpreted as a magnetic moment precessing around the external magnetic field.*

From the Lie algebraic point of view, these are SU(2) group action diagrams by the generators indicated in the central circles on the su(2) algebra. From the physical point of view, these diagrams are interpreted using spin state classification discussed in Section 4.2.3 – as rotations in the subspaces spanned by the two observables on the outside of the circle, generated by the operator that appears on the inside. Mathematically, the diagrams in Figure 10 describe the following propagator group orbits:

$$\begin{aligned} e^{-i\omega\mathbf{L}_Z t}\mathbf{L}_X e^{+i\omega\mathbf{L}_Z t} &= \mathbf{L}_X\cos(\omega t)+\mathbf{L}_Y\sin(\omega t)\\ e^{-i\omega\mathbf{L}_Z t}\mathbf{L}_Y e^{+i\omega\mathbf{L}_Z t} &= \mathbf{L}_Y\cos(\omega t)-\mathbf{L}_X\sin(\omega t)\\ e^{-i\omega\mathbf{L}_Z t}\mathbf{L}_Z e^{+i\omega\mathbf{L}_Z t} &= \mathbf{L}_Z \end{aligned} \tag{599}$$

but they may also be viewed (using the correspondence between operators and states discussed in Section 4.2.3) as rotations of the Cartesian components of the magnetic moment vector. This latter picture dominates chemistry literature, where only the observables are considered:

$$\begin{aligned} L_X &\xrightarrow{\omega\hat{L}_Z} L_X\cos(\omega t)+L_Y\sin(\omega t)\\ L_Y &\xrightarrow{\omega\hat{L}_Z} L_Y\cos(\omega t)-L_X\sin(\omega t)\\ L_Z &\xrightarrow{\omega\hat{L}_Z} L_Z \end{aligned} \tag{600}$$

The same rules apply to product states that involve other spins – because the Hamiltonian $\mathbf{H}=\omega\mathbf{L}_{\{X,Y,Z\}}$ commutes with operators acting on other spins, the same rotation diagrams apply to:

$$\cdots\otimes\mathbf{A}\otimes\mathbf{L}_{XYZ}\otimes\mathbf{B}\otimes\cdots \tag{601}$$

where the operators $\mathbf{A}$, $\mathbf{B}$, *etc.* on other spins are arbitrary. Because operators acting on different spins commute, the general case of the Zeeman interaction Hamiltonian being a linear combination of all single-spin operators in the system (Sections 3.1.6 and 3.2.12):

$$\mathbf{H}=\sum_k\vec{\mathbf{L}}^{(k)}\cdot\mathbf{Z}_k\cdot\vec{B} \tag{602}$$

reduces to the case considered above. Any exponential action by $\mathbf{H}$ splits into product of actions by single-spin operators (Section 4.3.2); those actions may be considered one at a time.

4.7.2 Evolution under spin-spin couplings

In the general case of an arbitrary interaction tensor, the product operator formalism offers no cognitive or logistical advantages over Liouville - von Neumann equation; brute-force numerics is the best way forward. However, in the common case of "weak" spin-spin coupling (Section 4.3.7.4), simple evolution diagrams do exist [125]. The weak interaction Hamiltonian is:

$$\mathbf{H}=\omega_C\mathbf{L}_Z\mathbf{S}_Z \tag{603}$$

where $\omega_C=2\pi J$ in the case of heteronuclear *J*-coupling. In the case of heteronuclear dipolar coupling, $\omega_C=-(\mu_0/4\pi)(\gamma_L\gamma_S\hbar/r_{LS}^5)\left[3(z_L-z_S)^2-r_{LS}^2\right]$, and so on for other interactions (Section 3.2).

The longitudinal magnetisation of both spins commutes with the Hamiltonian in Equation (603) and therefore remans invariant. The commutation relations for the transverse magnetisation are:

$$\begin{aligned} \left[\mathbf{L}_Z\mathbf{S}_Z,\mathbf{L}_X\right]&=\left[\mathbf{L}_Z,\mathbf{L}_X\right]\mathbf{S}_Z=+i\mathbf{L}_Y\mathbf{S}_Z, \qquad \left[\mathbf{L}_Z\mathbf{S}_Z,\mathbf{L}_Y\mathbf{S}_Z\right]=\left[\mathbf{L}_Z,\mathbf{L}_Y\right]\mathbf{S}_Z^2=-(i/4)\mathbf{L}_X\\ \left[\mathbf{L}_Z\mathbf{S}_Z,\mathbf{L}_Y\right]&=\left[\mathbf{L}_Z,\mathbf{L}_Y\right]\mathbf{S}_Z=-i\mathbf{L}_X\mathbf{S}_Z, \qquad \left[\mathbf{L}_Z\mathbf{S}_Z,\mathbf{L}_X\mathbf{S}_Z\right]=\left[\mathbf{L}_Z,\mathbf{L}_X\right]\mathbf{S}_Z^2=+(i/4)\mathbf{L}_Y \end{aligned} \tag{604}$$

where the factor of 4 in the denominators comes from $\hat{S}_Z^2 = \mathbf{1}/4$ for spin 1/2. For higher spin quantum numbers, the commutator would be different because $\hat{S}_Z^2$ would not be a multiple of the unit matrix; those cases are onerous, and numerical treatments are the best way forward.

With the commutators in place, Eq (596) yields the following equations of motion for the observables when both spins are 1/2:

$$\begin{cases} \dfrac{\partial}{\partial t} L_X = -\omega_C L_Y S_Z \\ \dfrac{\partial}{\partial t} L_Y S_Z = +\dfrac{\omega_C}{4} L_X \end{cases} \qquad \begin{cases} \dfrac{\partial}{\partial t} L_Y = +\omega_C L_X S_Z \\ \dfrac{\partial}{\partial t} L_X S_Z = -\dfrac{\omega_C}{4} L_Y \end{cases} \tag{605}$$

where angular brackets are now dropped, and the composite symbols like $L_Y S_Z$ are to be viewed as single variables, not products. The dynamics is again rotational, but the trajectories appear to be elliptical. For example, when the initial condition is L_X (left) or L_Y (right):

$$\begin{cases} L_X(t) = \cos(\omega_C t/2) \\ L_Y S_Z(t) = \frac{1}{2}\sin(\omega_C t/2) \end{cases} \qquad \begin{cases} L_Y(t) = \cos(\omega_C t/2) \\ L_X S_Z(t) = -\frac{1}{2}\sin(\omega_C t/2) \end{cases} \tag{606}$$

Moving the factor of 2 into the definition of the two-spin order turns ellipses into circles:

$$\begin{cases} L_X(t) = \cos(\omega_C t/2) \\ 2L_Y S_Z(t) = \sin(\omega_C t/2) \end{cases} \qquad \begin{cases} L_Y(t) = \cos(\omega_C t/2) \\ 2L_X S_Z(t) = -\sin(\omega_C t/2) \end{cases} \tag{607}$$

This normalisation transformation works fine in this system of two spin-1/2 particles, but becomes problematic in more general cases because the multipliers misbehave (Section 1.6.3.3) – a silly accounting trick of adding a non-interacting ghost spin at the other end of the Universe makes them change. Note also that the frequency is half of what occurs in the Hamiltonian in Eq (603). This may be fixed using the same normalisation trick – for example, for the weak *J*-coupling (Section 3.2.7) in NMR spectroscopy:

$$\mathbf{H} = \pi J\left(2\mathbf{L}_Z\mathbf{S}_Z\right) \tag{608}$$

and thus the rotation frequency is πJ. The corresponding rotation diagrams are:

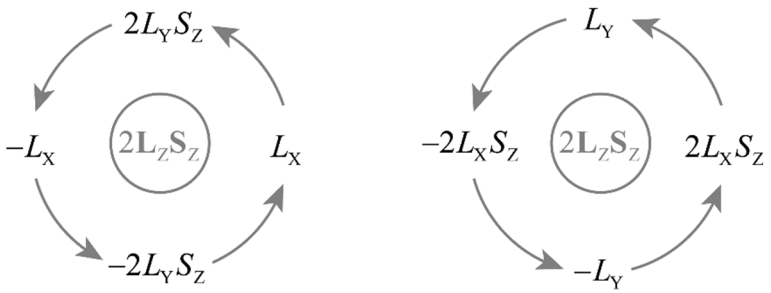

Figure 12. *Exponential action diagrams by SU(4) generator indicated in the circles on the su(4) Lie algebra. Physically, the indicated generator of SU(4) corresponds to the weak spin-spin coupling (Section 4.3.7.4), and this picture may therefore be interpreted as rotational dynamics between a transverse magnetisation direction of spin L and its perpendicular direction where the sign of the magnetisation depends on the longitudinal projection state of the partner spin S.*

Product operator formalism is well developed; instructions on dealing with more complicated systems and interactions may be found in [125]. There are *Mathematica* extensions that automate it [126].

The nature of direct product basis sets, and the following property of Kronecker products:

$$(\mathbf{A}\otimes\mathbf{B}\otimes\cdots)(\mathbf{C}\otimes\mathbf{D}\otimes\cdots)=(\mathbf{AC})\otimes(\mathbf{BD})\otimes\cdots \tag{609}$$

means that the evolution diagrams in Figures 11 and 12 apply to systems with an arbitrary number of spectator spins. Another extension appears when we notice that the exponential propagation relations in Eq (599) are the consequence of the commutation relations between the generators of $\mathfrak{su}(2)$ – any other system of operators that follows the same commutation rules as $\{\mathbf{S}_X,\mathbf{S}_Y,\mathbf{S}_Z\}$ would follow the same diagram as Figure 11. One example is Figure 12, and many more may be found in specialist literature.

4.7.3 Example: ideal pulse

Product operator formalism has pedagogic value – rigorous descriptions of magnetic resonance experiments may be smuggled into chemistry and biology departments because the use of quantum mechanics is not overt. It also helps make intuitive sense of complicated spin processes because dynamics on Lie algebras is mapped into what looks like rotational motion. A good example is evolution under strong radiofrequency or microwave pulses, where adjoint exponential action:

$$e^{-i\omega\mathbf{L}_Y t}\mathbf{L}_Z e^{+i\omega\mathbf{L}_Y t}=\mathbf{L}_Z\cos(\omega t)+\mathbf{L}_X\sin(\omega t) \tag{610}$$

requiring detailed knowledge of Chapter 1 material is represented by a three-dimensional rotation:

$$L_Z\xrightarrow{\omega\mathbf{L}_Y}L_Z\cos(\omega t)+L_X\sin(\omega t)\xrightarrow{\omega t=\pi/2}L_X \tag{611}$$

that is accessible to a liberal arts major. Here, the product of pulse frequency $\omega=-\gamma B_1$ and duration t is the flip angle. In magnetic resonance pulse sequence diagrams, it is common to specify ωt product in radians, and to leave the choice of B_1 and t to the user because equipment settings differ.

4.7.4 Example: spin echo

Product operator formalism provides a simple but rigorous description of the *spin echo* [127] – an important element of magnetic resonance experiments on heterogeneous samples, such as powders in solid state NMR and tissues in MRI, where the Larmor frequency ω_k may be different for each spin k in the ensemble. The pulse sequence contains two pulses and two delays:

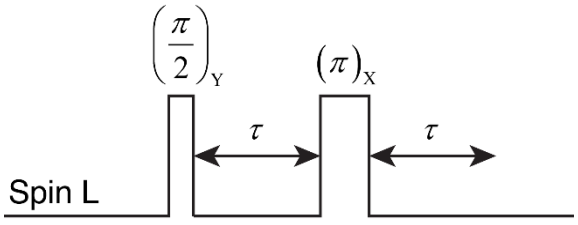

Figure 13. *One of the many possible spin echo experiments.*

where pulses are specified by their generator (X and Y subscripts correspond to $\mathbf{L}_X$ and $\mathbf{L}_Y$ evolution generators) and the effective flip angle $\varphi=-\gamma B_1 t$, where t is the duration of the pulse. If the initial condition is Z magnetisation, then Figure 10 indicates that, at the end of the first pulse:

$$L_Z^{(k)}\xrightarrow{(\pi/2)_Y}L_Z^{(k)}\cos\left(\frac{\pi}{2}\right)+L_X^{(k)}\sin\left(\frac{\pi}{2}\right)=L_X^{(k)} \tag{612}$$

where $(\pi/2)_Y$ is a shorthand for the evolution under $\omega\mathbf{L}_Y$ for a time t such that $\omega t=\pi/2$. The system is now in the state $\sum_k\mathbf{L}_X^{(k)}$ – all spins have the same phase. However, because their precession frequencies are different, they would go out of phase during the evolution period τ:

$$L_{\mathrm{X}}^{(k)} \xrightarrow{\omega_k \mathbf{L}_{\mathrm{Z}}^{(k)}} L_{\mathrm{X}}^{(k)} \cos\left(\omega_k \tau\right) + L_{\mathrm{Y}}^{(k)} \sin\left(\omega_k \tau\right) \tag{613}$$

This can be undesirable, for example in MRI, because the total transverse magnetisation is reduced when there is a distribution in the transverse precession phases. However, this dephasing is reversed after the π_{X} pulse is applied, which flips the signs of $L_{\mathrm{Y}}^{(k)}$:

$$L_{\mathrm{X}}^{(k)} \cos\left(\omega_k \tau\right) + L_{\mathrm{Y}}^{(k)} \sin\left(\omega_k \tau\right) \xrightarrow{\pi_{\mathrm{X}}} L_{\mathrm{X}}^{(k)} \cos\left(\omega_k \tau\right) - L_{\mathrm{Y}}^{(k)} \sin\left(\omega_k \tau\right) \tag{614}$$

Then, at the end of the second evolution period τ:

$$\begin{aligned} L_{\mathrm{X}}^{(k)} \cos\left(\omega_k \tau\right) - L_{\mathrm{Y}}^{(k)} \sin\left(\omega_k \tau\right) \xrightarrow{\omega \mathbf{L}_{\mathrm{Z}}^{(k)}} & \left[L_{\mathrm{X}}^{(k)} \cos\left(\omega_k \tau\right) + L_{\mathrm{Y}}^{(k)} \sin\left(\omega_k \tau\right)\right] \cos\left(\omega_k \tau\right) - \\ & \left[L_{\mathrm{Y}}^{(k)} \cos\left(\omega_k \tau\right) - L_{\mathrm{X}}^{(k)} \sin\left(\omega_k \tau\right)\right] \sin\left(\omega_k \tau\right) = \\ & = L_{\mathrm{X}}^{(k)} \left[\cos^2\left(\omega_k \tau\right) + \sin^2\left(\omega_k \tau\right)\right] = L_{\mathrm{X}}^{(k)} \end{aligned} \tag{615}$$

where the magnetisation is again frequency-independent – all spins have the same phase. The π pulse of the spin echo experiment is called *refocussing pulse* because its effect is to bring the ensemble magnetisation back into a coherent state.

4.7.5 Example: magnetisation transfer

A popular building block of magnetic resonance experiments is magnetisation transfer through weak scalar coupling [128]. Consider a liquid state sample containing ^{1}H–^{15}N spin pairs in a high-field magnet, and an experiment in which two independent RF transmitters are tuned exactly to ^{1}H and ^{15}N Zeeman frequencies. These transmitters are assumed to be powerful enough that millisecond-scale *J*-coupling evolution may be ignored during microsecond-scale RF pulses. In the rotating frame, the Hamiltonian is:

$$\mathbf{H} = \begin{cases} \omega_{\mathrm{1L}} \left(\mathbf{L}_{\mathrm{X}} \cos\varphi_{\mathrm{L}} + \mathbf{L}_{\mathrm{Y}} \sin\varphi_{\mathrm{L}}\right) + \omega_{\mathrm{1S}} \left(\mathbf{S}_{\mathrm{X}} \cos\varphi_{\mathrm{S}} + \mathbf{S}_{\mathrm{Y}} \sin\varphi_{\mathrm{S}}\right) & \text{during hard pulses} \\ \omega_{\mathrm{C}} \mathbf{L}_{\mathrm{Z}} \mathbf{S}_{\mathrm{Z}}, \quad \omega_{\mathrm{C}} = 2\pi J & \text{during free evolution} \end{cases} \tag{616}$$

where $\omega_{\mathrm{1L,1S}}$ are nutation frequencies under the pulses applied to the indicated spins, $\varphi_{\mathrm{L,S}}$ are phases of those pulses in the rotating frame, and ω_{C} is the angular frequency of the scalar coupling. Full quantum mechanical treatment of the following pulse sequence

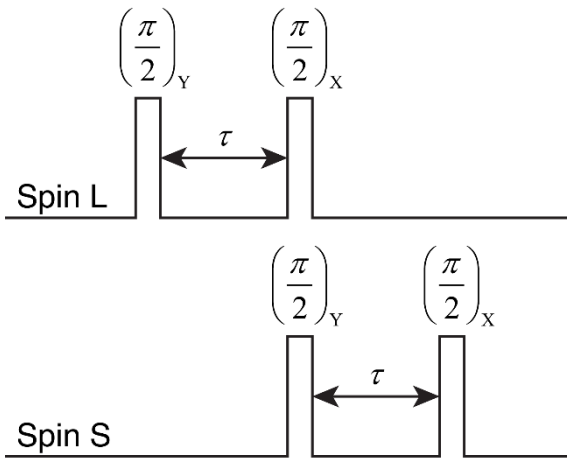

Figure 14. *A magnetisation transfer pulse sequence that converts longitudinal magnetisation of spin L into longitudinal magnetisation on spin S in a system where both spins are exactly on resonance with their corresponding control channel transmitters and the spin-spin coupling is "weak" in the sense of only having the ZZ term (Section 4.3.8.4).*

either analytically or numerically would be a considerable undertaking, but product operator formalism makes the analysis straightforward.

Consider the initial condition where protons (L spin) are magnetised on the Z axis, but the initial magnetisation of ^{15}N (S spin) is negligible; thus $\boldsymbol{\rho}_0 \propto \mathbf{L}_Z$ in the high-temperature limit (Section 6.9). The first pulse makes proton magnetisation transverse (middle diagram in Figure 11):

$$L_Z \xrightarrow{(\pi/2)_Y} L_X \tag{617}$$

Subsequent evolution under $\omega_C \mathbf{L}_Z \mathbf{S}_Z$ rotates L_X towards the two-spin order (left diagram in Figure 12). Choosing a delay τ such that $\omega_C \tau = \pi$ brings the magnetisation completely into the two-spin order:

$$L_X \xrightarrow{\omega_C \mathbf{L}_Z \mathbf{S}_Z} L_X \cos\left(\frac{\omega_C}{2}\tau\right) + 2L_Y S_Z \sin\left(\frac{\omega_C}{2}\tau\right) \xrightarrow{a\tau=\pi} 2L_Y S_Z \tag{618}$$

The next pair of pulses moves the state where the proton is transverse and nitrogen longitudinal into the state where the proton is longitudinal, and the nitrogen is transverse:

$$2L_Y S_Z \xrightarrow{(\pi/2)_X \text{ on } L} 2L_Z S_Z \xrightarrow{(\pi/2)_Y \text{ on } S} 2L_Z S_X \tag{619}$$

The next evolution period (right diagram in Figure 12) rotates the resulting two-spin order towards transverse nitrogen magnetisation. Choosing again the evolution delay such that $\omega_C \tau = \pi$ yields:

$$2L_Z S_X \xrightarrow{\omega_C \mathbf{L}_Z \mathbf{S}_Z} 2L_Z S_X \cos\left(\frac{\omega_C}{2}\tau\right) + S_Y \sin\left(\frac{\omega_C}{2}\tau\right) \xrightarrow{\omega_C \tau=\pi} S_Y \tag{620}$$

The optional last pulse (left diagram in Figure 11) makes nitrogen magnetisation longitudinal:

$$S_Y \xrightarrow{(\pi/2)_X \text{ on } S} S_Z \tag{621}$$

If the two nuclei are not exactly on resonance with the rotating frames, or there exists a distribution of precession frequencies, spin echo stages – in the form of π pulses – are inserted into the evolution periods to make sure that the offsets are refocused.

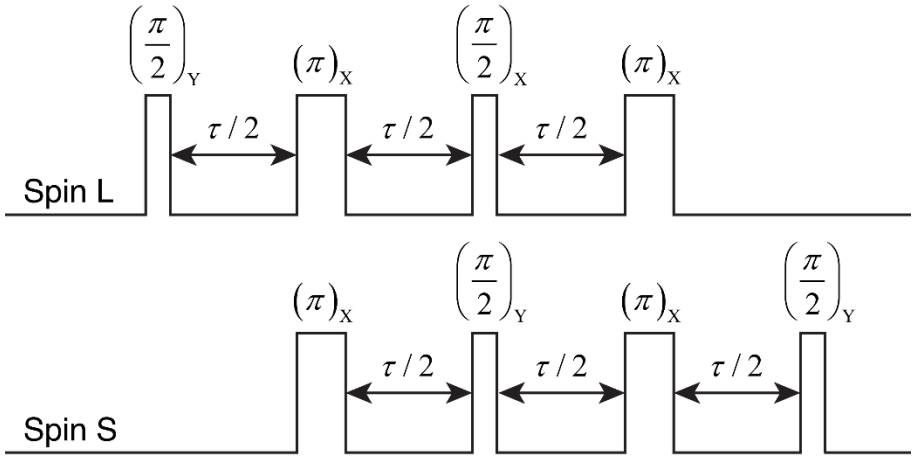

Figure 15. *A magnetisation transfer pulse sequence that converts longitudinal magnetisation of spin L into longitudinal magnetisation on spin S in a system where spins might not be on resonance with their corresponding control channel transmitters and the spin-spin coupling is "weak" in the sense of only having the ZZ term (Section 4.3.8.4).*

A similar analysis shows that this sequence accomplishes the same magnetisation transfer, but it is also resilient to Larmor frequency offsets on both spins.